AFRL-RY-HS-TR-2010-0023

Scattering of Electromagnetic Waves in the Presence of Wave Turbulence Excited by a Flow with Velocity Shear

Vladimir Sotnikov,
University of Nevada at Reno
Reno, NV 89506

Jean-Noel Leboeuf
JNL Scientific
Casa Granda, AZ 85194

Saba Mudaliar
Air Force Research Laboratory
Sensors Directorate
Hanscom AFB MA 01731

19 March 2010

Final Report

AIR FORCE RESEARCH LABORATORY
Sensors Directorate
Electromagnetics Technology Division
80 Scott Drive
Hanscom AFB MA 01731-2909

NOTICE AND SIGNATURE PAGE

Distribution: Unlimited, Statement A

NOTICE

USING GOVERNMENT DRAWINGS, SPECIFICATIONS, OR OTHER DATA INCLUDED IN THIS DOCUMENT FOR ANY PURPOSE OTHER THAN GOVERNMENT PROCUREMENT DOES NOT IN ANY WAY OBLIGATE THE US GOVERNMENT. THE FACT THAT THE GOVERNMENT FORMULATED OR SUPPLIED THE DRAWINGS, SPECIFICATIONS, OR OTHER DATA DOES NOT LICENSE THE HOLDER OR ANY OTHER PERSON OR CORPORATION; OR CONVEY ANY RIGHTS OR PERMISSION TO MANUFACTURE, USE, OR SELL ANY PATENTED INVENTION THAT MAY RELATE TO THEM.

THIS TECHNICAL REPORT WAS CLEARED FOR PUBLIC RELEASE BY THE ELECTRONICS SYSTEMS CENTER PUBLIC AFFAIRS OFFICE FOR THE AIR FORCE RESEARCH LABORATORY ELECTROMAGNETICS TECHNOLOGY DIVISION AND IS AVAILABLE TO THE GENERAL PUBLIC, INCLUDING FOREIGN NATIONALS. COPIES MAY BE OBTAINED FROM THE DEFENSE TECHNICAL INFROMATION CENTER (DTIC) (http://www.dtic.mil)

AFRL-RY-HS-TR-2010-0023 HAS BEEN REVIEWED AND IS APPROVED FOR PUBLICATION IN ACCORDANCE WITH ASSIGNED DISTRIBUTION STATEMENT.

Saba Mudaliar

SABA MUDALIAR
Electronics Engineer
Electromagnetic Scattering Branch

Bertus Weijers

BERTUS WEIJERS
Branch Chief
Electromagnetic Scattering Branch

Robert V. McGahan

ROBERT V. McGAHAN
Technical Communication Advisor
Electromagnetics Technology Division

This report is published in the interest of scientific and technical information exchange and does not constitute the Government's approval or disapproval of its ideas or findings.

REPORT DOCUMENTATION PAGE

Form Approved
OMB No. 0704-0188

PLEASE DO NOT RETURN YOUR FORM TO THE ABOVE ADDRESS.

1. REPORT DATE *(DD-MM-YYYY)*	2. REPORT TYPE	3. DATES COVERED *(From - To)*
02-03-2010	Final Report	27 Feb 2008 - 27 Feb 2010

4. TITLE AND SUBTITLE

Scattering of electromagnetic waves in the presence of wave turbulence excited by a flow with velocity shear

5a. CONTRACT NUMBER

FA8718-08-C-0003

5b. GRANT NUMBER

N/A

5c. PROGRAM ELEMENT NUMBER

61102F

6. AUTHOR(S)

1) V.I. Sotnikov, Department of Physics, University of Nevada, Reno NV
2) J.N. Leboeuf, JNL Scientific, Casa Grande AZ
3) S. Mudaliar, AFRL, Sensors Directorate, Hanscom AFB MA

5d. PROJECT NUMBER

4916

5e. TASK NUMBER

HE

5f. WORK UNIT NUMBER

03

7. PERFORMING ORGANIZATION NAME(S) AND ADDRESS(ES)

1) Dept. of Physics
University of Nevada
5625 Fox Ave.
Reno, NV 89557-0058

2) JNL Scientific
2428 East Antigua Drive
Casa Grande, AZ 85194

3) Air Force Research Laboratory
Sensors Directorate
80 Scott Drive
Hanscom AFB, MA 01731

8. PERFORMING ORGANIZATION REPORT NUMBER

N/A

9. SPONSORING/MONITORING AGENCY NAME(S) AND ADDRESS(ES)

Electromagnetic Technology Division
Sensors Directorate
Air Force Research Laboratory
80 Scott Drive, Hanscom AFB, MA 01731-2909

10. SPONSOR/MONITOR'S ACRONYM(S)

AFRL-RY-HS

11. SPONSOR/MONITOR'S REPORT NUMBER(S)

AFRL-RY-HS-TR-2010-0023

12. DISTRIBUTION/AVAILABILITY STATEMENT

Distribution A / Approved for Public Release by ESC PA # 66ABW-2009-1347

13. SUPPLEMENTARY NOTES

14. ABSTRACT

It is well-known that an incompressible sheared flow with an inflection point in the velocity profile will result in the formation of turbulent vortices. In the case of compressible plasma flow with velocity shear ion acoustic fluctuations in addition to vortices will be generated. We present a detailed analysis of the excitation of such low frequency oscillations in a compressible plasma flow with velocity shear. To examine the process of excitation and nonlinear saturation of low frequency oscillations in the presence of a flow shear a nonlinear system of equations was derived. We employ a predictor-corrector method to solve this system numerically. Spectral analysis of the numerical solutions allows us to calculate the turbulent density spectra for different velocity profiles. We find that the impact of this turbulence associated with ion-acoustic wave fluctuations is considerably more significant and dominant than that due to turbulent vortices. On employing a single scattering perturbation theory we observe that the electromagnetic scattering from the turbulent density fluctuations of the flow results in shifted signal spectra above and below that of the source.

15. SUBJECT TERMS

Flow shear, ion acoustic turbulence, wave scattering

16. SECURITY CLASSIFICATION OF:			17. LIMITATION OF ABSTRACT	18. NUMBER OF PAGES	19a. NAME OF RESPONSIBLE PERSON
a. REPORT	b. ABSTRACT	c. THIS PAGE			Saba Mudaliar
U	U	U	UU	27	19b. TELEPHONE NUMBER *(Include area code)*

Reset

Standard Form 298 (Rev. 8/98)
Prescribed by ANSI Std. Z39.18

Table of Contents

List of Figures

1. INTRODUCTION

The problem of electromagnetic (EM) wave scattering for waves propagating through a plasma sheath surrounding reentry vehicles and vehicles traveling at hypersonic velocities at high altitudes has attracted the attention of many researchers [1-4]. In this report the influence of low frequency wave turbulence excited in a compressible supersonic plasma flow with velocity shear around a vehicle is analyzed. A system of nonlinear equations consisting of the momentum equations for ions, the mass conservation equations for ions and electrons, and an equation for the density of adiabatic electrons is presented. These equations are complemented by the Poisson equation for the electrostatic potential associated with the excitation of ion acoustic perturbations due to the presence of the flow shear. Our equations appropriately take into consideration the effects of ion-neutral collisions and ion viscosity. This system of equations is solved numerically and wave spectra of excited low frequency perturbations are obtained. We investigate the interaction of the incident EM wave and low frequency turbulent pulsations inside a plasma sheath, considering them relatively small. In this case we can separate incident and scattered waves. At the same time characterizing the interaction of the incident wave with the turbulent plasma pulsations requires the use of nonlinear equations [5, 6]. The nonlinear current generated by this process in the case of a high frequency incident EM wave contains only the electron component. On analyzing the dispersion equation for electromagnetic, electrostatic Langmuir, and ion acoustic waves involved in the scattering process, we find that different types of scattering scenarios are possible. In the case when the frequency of the EM signal is much greater than the electron plasma frequency ($\omega_0 >> \omega_{pe}$), the scattered waves will also be electromagnetic with frequency $\omega_0 \pm \omega_A$, where ω_A is the frequency of the ion acoustic wave generated by the excited turbulent wave spectrum. In the case when the frequency of the incident EM signal is close to the electron plasma frequency ($\omega_0 \geq \omega_{pe}$), two processes can take place:

1. Scattering of the incident EM signal into another EM wave with the frequency $\omega_0 \pm \omega_A$.

2. Transformation of the incident EM signal into a Langmuir wave with frequencies in the range $\omega_0 \pm \omega_A$.

We find that turbulence caused by such ion acoustic wave instabilities can strongly influence the properties of electromagnetic waves, potentially impacting the quality of communication channels.

The following is the layout of this report. In Section II, we present the multi-fluid equations underlying our linear stability analysis and the nonlinear saturation stage of the instability associated with a velocity shear in the plasma flow. In Section III we discuss numerical solutions of the nonlinear equations including a description of the spectra of generated density perturbations associated with the ion acoustic waves. In Section IV we analyze the scattering of the incident EM wave on the electron density perturbations and calculate the amplitudes of the scattered waves and scattering cross sections for the two cases described above. We conclude the report with a summary and a discussion of the main results.

2. INSTABILITY OF A PLASMA FLOW WITH A VELOCITY SHEAR

In the present section we investigate the excitation of vortices and ion acoustic type perturbations in a compressible supersonic plasma flow with velocity shear. A system of nonlinear equations consisting of the momentum equations for ions, the mass conservation equations for ions and electrons, and an equation for the density of adiabatic electrons is presented below. These equations are complemented by the Poisson equation for the electrostatic potential associated with the excitation of ion acoustic perturbations due to the presence of the flow shear. Equations presented below also properly take into consideration the effects of ion-neutral collisions and ion viscosity. We are interested in the excitation of turbulent pulsations in a compressible supersonic plasma flow with velocity shear in the two-dimensional case (see Figure 1 below).

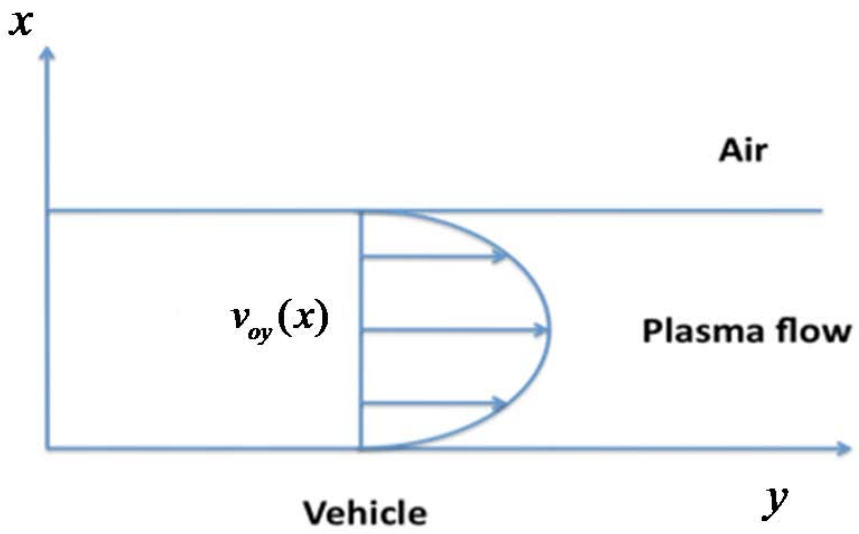

Fig. 1. Plasma flow has velocity $\mathbf{v}_{0y}(x)$ directed along the *y* axis and velocity shear is along the *x* axis.

The basic equations which describe the plasma flow are as follows:

1. Equation of motion for the ions:

$$m_i n_i \left\{ \frac{\partial \mathbf{v}_i}{\partial t} + (\mathbf{v}_i \cdot \vec{\nabla}) \mathbf{v}_i \right\} = -Z e n_i \vec{\nabla} \varphi - \vec{\nabla} P_i + m_i n_i \nu_i \Delta \mathbf{v}_i - \mu_{ia} n_i \nu_{ia} (\mathbf{v}_i - \mathbf{v}_a) \tag{1}$$

2. Equation for the adiabatic electrons:

$$T_e \vec{\nabla} n_e = e n_e \vec{\nabla} \varphi \tag{2}$$

3. Mass conservation equation for the ions:

$$\frac{\partial n_i}{\partial t} + div(n_i \mathbf{v}_i) = 0 \tag{3}$$

4. Poisson equation for the electrostatic potential:

$$\Delta \varphi = 4\pi e (n_e - n_i) \tag{4}$$

In equations (1)-(4) the flow velocity can be presented in the following form:

$$\mathbf{v}_{\mathrm{i}} = v_{0y}(x)\mathbf{e}_y + \delta\mathbf{v}_{\mathrm{i}}(x,y,t) \tag{5}$$

In equation (5) $\mathbf{v}_{0y}(x)$ is the initial flow velocity, which varies along the direction perpendicular to the flow direction, and $\delta\vec{\mathrm{v}}_i(t,x,y)$ are the perturbed velocities which appear due to excitation of vortices and ion acoustic oscillations inside the plasma flow.

To solve (1)-(4) numerically and to find excited density and electric field perturbations and their spectra we first introduce dimensionless variables and rewrite the system of equations in dimensionless form. For the ion dimensional mass density $\tilde{\rho}_i$ and dimensional number density $\tilde{N}_i$ we introduce dimensionless mass ρ_i and number densities N_i as

$$\tilde{\rho}_i(\tilde{x},\tilde{y}) = \tilde{\rho}_{0\max}\,\rho_i(x,y) \qquad \tilde{N}_{\mathrm{i}} = \tilde{n}_{0\max}\,N_{\mathrm{i}}(x,y) \qquad \tilde{\rho}_{0\max} = \tilde{M}_i\tilde{n}_{0\max} \tag{6}$$

where $\tilde{\rho}_{0\max}$ and $\tilde{n}_{0\max}$ are maximum dimensional mass and number densities and $\tilde{M}_i$ is the dimensional ion mass.

Now we introduce dimensionless time according to

$$t = \tilde{\omega}_{pi}\tilde{t}\,, \tag{7}$$

where the dimensional ion plasma frequency is given by

$$\tilde{\omega}_{pi} = \sqrt{\frac{4\pi Z^2 e^2 \tilde{n}_{0i\max}}{M_i}}\,, \tag{8}$$

and $\tilde{t}$ is dimensional time.

We normalize the space variables as

$$\tilde{x} = \tilde{\Delta}_i x \qquad \tilde{\mathrm{y}} = \tilde{\Delta}_i y\,, \tag{9}$$

where $\tilde{\Delta}_i$ is the distance between two grid points.

For the dimensionless ion velocity in the flow we use

$$\vec{\tilde{u}}_{\mathrm{i}}(\tilde{x},\tilde{y}) = \tilde{\omega}_{pi}\tilde{\Delta}_{\mathrm{i}}\vec{u}_{\mathrm{i}}(x,y)\,. \tag{10}$$

For the dimensionless electrostatic potential of the excited perturbations we introduce

$$\tilde{\Phi}(\tilde{x},\tilde{y})=\frac{\tilde{\mathrm{M}}_{\mathrm{i}}\tilde{\omega}_{pi}^{2}\tilde{\Delta}_{i}^{2}}{Z\tilde{e}}\Phi(x,y)\ . \tag{11}$$

Finally, for the dimensionless mass and number density we use

$$\rho_{\mathrm{i}}=\frac{\tilde{\rho}_{\mathrm{i}}}{\tilde{\rho}_{0\max}}=\frac{\tilde{\mathrm{N}}_{\mathrm{i}}}{\tilde{n}_{0\max}}=\mathrm{N}_{\mathrm{i}}\,. \tag{12}$$

Now we can rewrite the main system of Equations 1–4 in the dimensionless and conservative form as follows:

Momentum equations:

$$\begin{aligned}&\frac{\partial(N_i u_{ix})}{\partial t}+\frac{\partial}{\partial x}(N_i u_{ix}u_{ix})+\frac{\partial}{\partial y}(N_i u_{ix}u_{iy})=\\&\quad=-N_i\frac{\partial\Phi}{\partial x}-\frac{\tilde{r}_{Di}^{2}}{\tilde{\Delta}_i^{2}}\frac{\partial N_i}{\partial x}-\frac{\tilde{\mu}_{in}}{\tilde{m}_i}\frac{\tilde{\nu}_{in}}{\tilde{\omega}_{pi}}N_i(u_{ix}-u_{nx})+\frac{\tilde{\nu}_i}{\tilde{\omega}_{pi}\tilde{\Delta}_i^{2}}N_i\left(\frac{\partial^2}{\partial x^2}+\frac{\partial^2}{\partial y^2}\right)u_{ix}\end{aligned} \tag{13}$$

$$\begin{aligned}&\frac{\partial(N_i u_{iy})}{\partial t}+\frac{\partial}{\partial x}(N_i u_{iy}u_{ix})+\frac{\partial}{\partial y}(N_i u_{iy}u_{iy})=\\&\quad=-N_i\frac{\partial\Phi}{\partial y}-\frac{\tilde{r}_{Di}^{2}}{\tilde{\Delta}_i^{2}}\frac{\partial N_i}{\partial y}-\frac{\tilde{\mu}_{in}}{\tilde{m}_i}\frac{\tilde{\nu}_{in}}{\tilde{\omega}_{pi}}N_i(u_{iy}-u_{ny})+\frac{\tilde{\nu}_i}{\tilde{\omega}_{pi}\tilde{\Delta}_i^{2}}N_i\left(\frac{\partial^2}{\partial x^2}+\frac{\partial^2}{\partial y^2}\right)u_{iy}\end{aligned} \tag{14}$$

Mass conservation equation:

$$\frac{\partial N_i}{\partial t}+\frac{\partial}{\partial x}(N_i u_{ix})+\frac{\partial}{\partial y}(N_i u_{iy})=0 \tag{15}$$

Poisson equation:

$$\Delta\Phi=\frac{1}{Z}(Z-N_i)+\frac{1}{Z}\frac{\tilde{\omega}_{pi}^{2}}{(\tilde{T}_e/\tilde{M}_i)}\tilde{\Delta}_i^{2}\Phi \tag{16}$$

Equation for adiabatic electrons:

$$\tilde{N}_e=\tilde{N}_{0e}\left\{\exp\left(\frac{\tilde{e}\tilde{\Phi}}{\tilde{T}_e}\right)-1\right\}=\tilde{N}_{0e}\frac{\tilde{e}\tilde{\Phi}}{\tilde{T}_e}=\tilde{N}_{0e}\frac{\tilde{M}_i\tilde{\omega}_{pi}^{2}\tilde{\Delta}_i^{2}}{Z\tilde{T}_e}\Phi \tag{17}$$

In Equations 13–17 we also used:

$$\tilde{N}_e=Z\tilde{N}_i\qquad\tilde{\omega}_{pi}^{2}=\frac{4\pi Z^{2}\tilde{e}^{2}\tilde{N}_i}{\tilde{M}_i}\ , \tag{18}$$

where Z is the charge number of ions.

Using the above dimensionless system of equations we investigate the linear and nonlinear stages of

1. Vortices with $\nabla \times \mathbf{v} \neq 0$
2. Ion acoustic fluctuations.

We choose the following Gaussian initial velocity profile (see Figure 2):

$$v_{0y}(x) = \exp\left\{-\frac{(x - x_{mid})^2}{2x_{wid}^2}\right\} \tag{19}$$

where $x_{mid} = \frac{1}{2} L_x$, $x_{wid} = \frac{1}{8} L_x$, and L_x is the size of the simulation box in the x direction. Note that this profile has inflection points (a necessary condition for the excitation of vortices) and it can also be responsible for the excitation of ion acoustic waves inside the plasma flow.

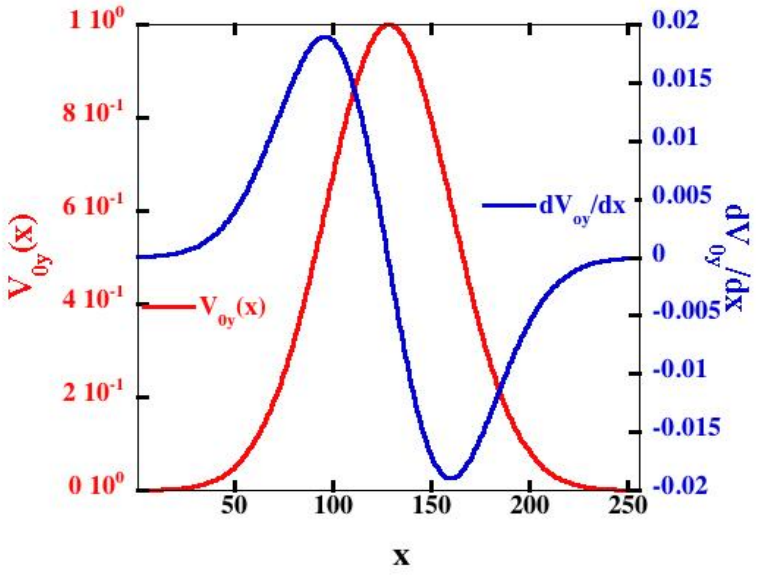

Fig. 2. Gaussian initial velocity profile (red) and its derivative (blue) for the dimensionless speed.

Below we present an algorithm for the numerical solution of the system of Equations 13–17 initialized with the Gaussian flow velocity profile (see Equation 19). The dimensionless time evolution equations are solved using temporal and spatial finite

differences. They are integrated in time using a robust two-step predictor corrector with an optional Lax step in the predictor [7, 8]. The time integration scheme is illustrated here using the density equation, where the density is denoted by N and the superscripts denote time levels as $n*\Delta t$ (or just * for the predictor step time index) and the subscripts spatial locations as $i*\Delta x$ and $j*\Delta y$, where Δs indicate the unit steps in time and space.

Predictor:

$$\begin{aligned} N^{*}_{i,j} = \left\langle N^{n}_{i,j} \right\rangle &- \left(0.5*\Delta t\right)\times\left\{\tfrac{1}{2}\left[\left(NV_x\right)^{n}_{i+1,j} - \left(NV_x\right)^{n}_{i-1,j}\right]\right\} \\ &- \left(0.5*\Delta t\right)\times\left\{\tfrac{1}{2}\left[\left(NV_x\right)^{n}_{i,j+1} - \left(NV_x\right)^{n}_{i,j-1}\right]\right\} \\ &- \left(0.5*\Delta t\right)\times D\times\left\{N^{n}_{i+1,j} - 2*N^{n}_{i,j} + N^{n}_{i-1,j}\right\} \\ &- \left(0.5*\Delta t\right)\times D\times\left\{N^{n}_{i,j+1} - 2*N^{n}_{i,j} + N^{n}_{i,j-1}\right\} \end{aligned} \tag{20}$$

Optional Lax Step in Predictor:

Lax: $\left\langle N^{n}_{i,j} \right\rangle = \tfrac{1}{4}\left[N^{n}_{i+1,j} + N^{n}_{i-1,j} + N^{n}_{i,j+1} + N^{n}_{i,j-1}\right]$

No Lax: $\left\langle N^{n}_{i,j} \right\rangle = N^{n}_{i,j}$

Corrector:

$$\begin{aligned} N^{n+1}_{i,j} = N^{n}_{i,j} &- \Delta t\times\left\{\tfrac{1}{2}\left[\left(NV_x\right)^{*}_{i+1,j} - \left(NV_x\right)^{*}_{i-1,j}\right]\right\} \\ &- \left(\Delta t\right)\times\left\{\tfrac{1}{2}\left[\left(NV_x\right)^{*}_{i,j+1} - \left(NV_x\right)^{*}_{i,j-1}\right]\right\} \\ &- \left(\Delta t\right)\times D\times\left\{N^{n}_{i+1,j} - 2*N^{n}_{i,j} + N^{n}_{i-1,j}\right\} \\ &- \left(\Delta t\right)\times D\times\left\{N^{n}_{i,j+1} - 2*N^{n}_{i,j} + N^{n}_{i,j-1}\right\} \end{aligned} \tag{21}$$

Note that diffusion acts only on the perturbed part of the density.

One unique feature of our numerical algorithm is the use of well-established templates which are repeatedly employed to perform first and second derivatives in space-centered finite difference form in both the *x* and *y* directions. These are the only derivatives used,

given the conservative formulation of the convective nonlinearities in all three dynamical equations. Also, the Poisson equation is solved using Fast Fourier Transforms as incorporated in the FFT2 set of routines long used in particle-in-cell codes developed over many decades at UCLA [9]. Thus the Poisson equation reduces to

$$\Phi_k = \left\{ k^2 + \frac{T_i}{T_e} \right\}^{-1} n_k , \tag{22}$$

with n_k representing the perturbed density in *k*-space only and its multiplier constituting the so-called form factor where an appropriate digital filter can be incorporated if needed. Furthermore, a dynamic time step of integration has been implemented in our algorithm whereby the instantaneous time step is adjusted to the inverse of one-half of the maximum *x* or *y* velocity anywhere on the grid thereby insuring that the Courant stability and accuracy condition [7, 8] is satisfied at all time in the nonlinear calculations. Boundary conditions other than periodic (and even periodic for ease of testing of the bounded implementation) have been incorporated in our algorithm using the image charge method [10]. This means that the appropriate image system is replicated from the physical one with the correct parity. As an illustration, if the derivative of the density is to go to zero at the physical boundary or, put in another way, if the density is continuous across that boundary, then the density in the image system is such that

$$N(2L_x - x) = +N(x). \tag{23}$$

Periodic boundary conditions imposed over the extended system result in

$$N(L_x + x) = +N(x) \ , \tag{24}$$

whereas density going to zero at the wall would look like:

$$N(2L_x - x) = +N(x). \tag{25}$$

So doing, the boundary is actually between the last grid point in the physical system and the first grid point in the image system taking the right-most boundary as an example. The parity for the other terms in the equations consistently follows from the choice made for *N*. Even though the image method results in twice the expense, it is much to be desired for symmetric boundary conditions (i.e. the same boundary conditions imposed at both boundaries) because of its simplicity and ease of implementation. Results below are for the flow-driven ion acoustic instability, with uniform density and Gaussian velocity

profile, and T_e=T_i=1.0. The parameters are such that $V_{Ti} = \omega_{pi} \times \tilde{\Delta}_i$. With T_e=T_i it also follows that the unit grid spacing $\tilde{\Delta}_i = r_{De}$ where r_{De} is the Debye radius of electrons.

The plots below (Figures 3-6) are for maximum flow speed equal to 2.5 times the speed of sound:

$$u_{0\max} = 2.5 \times C_S \quad . \tag{26}$$

In Figure 3 the excitation of ion acoustic oscillations by a flow with a velocity shear in the form of a Gaussian profile is presented. The black curve corresponds to the normalized kinetic energy of the flow. The blue and red curves correspond to dimensionless density and electrostatic potential versus dimensionless time, respectively.

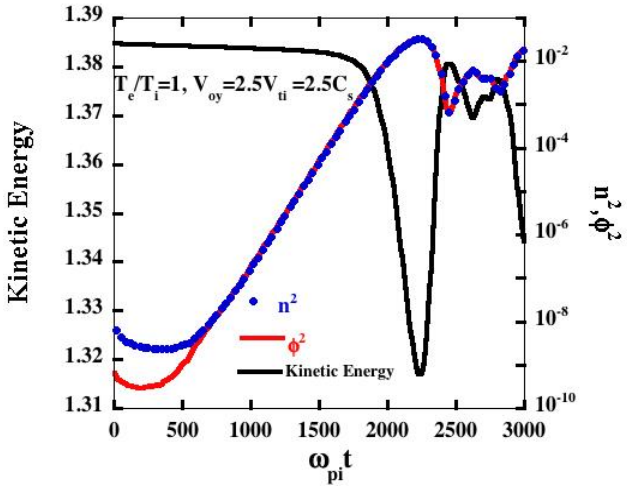

Fig. 3. The black curve corresponds to the normalized kinetic energy of the flow. The blue and red curves correspond to dimensionless density and electrostatic potential versus dimensionless time, respectively.

It is clear that the source of the energy for the instability development is the kinetic energy of the plasma flow. Ion density and electrostatic potential have the same growth rate. Saturation of instability in the nonlinear stage is connected with ion dissipation.

Growing perturbations of the electrostatic potential Φ at different moments in time are presented in Figures 4 and 5. According to Equation 17 the electron density perturbation N_e follows the perturbations of the potential.

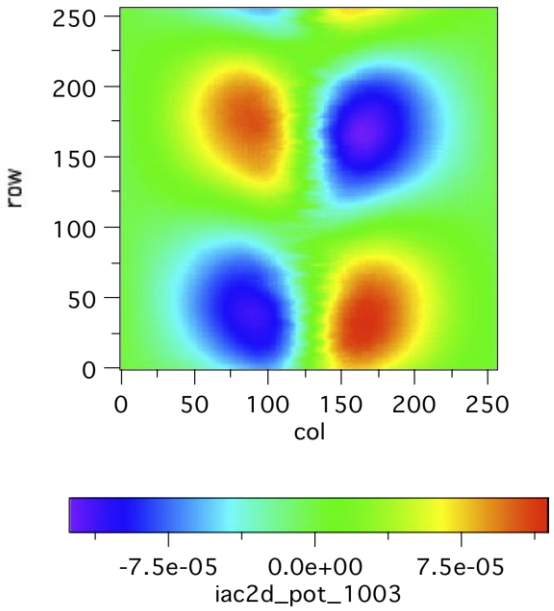

Fig. 4. Potential at $\omega_{pi}t = 900$

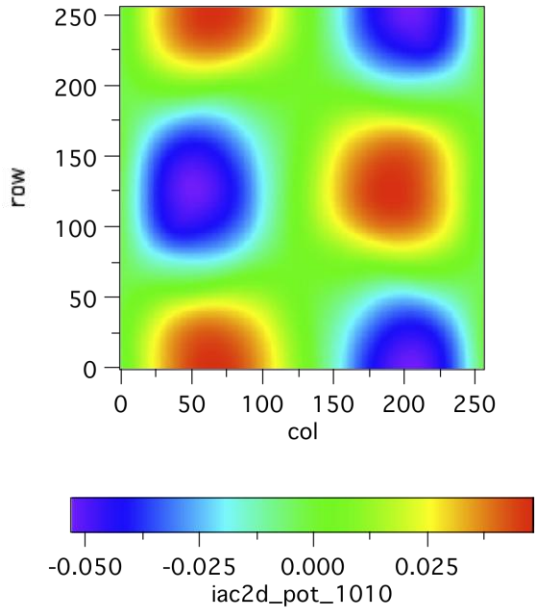

Fig. 5. Potential at $\omega_{pi}t = 3000$

The formation of large scale structures in the potential can be observed in Figure 5. Note that these density structures are centered in the regions of maximum velocity gradient, associated with the Gaussian velocity profile. In Figure 6, the k_x and k_y spectra of the density fluctuations are presented. The decay index α of the amplitude of the density fluctuations with respect to normalized k_x and k_y is found to be within the interval $-2.15 < \alpha < -1.98$.

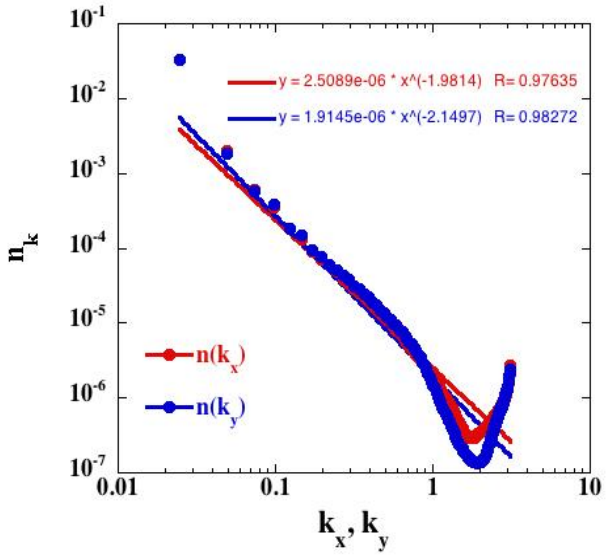

Fig. 6. Spectra in k_x and k_y of the density fluctuations

The results of the spectrum analysis also show that the decay index of the *k*-spectrum is highly dependent on the temperature ratio T_e/T_i and on the maximum of the flow velocity $u_{0\max}$.

3. ELECTROMAGNETIC WAVE SCATTERING

Below we present an analysis of the scattering of EM waves on density perturbations associated with ion acoustic turbulence excited by a plasma flow with velocity shear. The

amplitudes and spectra of the scattered waves, as well as the scattering cross section for the EM wave propagating through the plasma sheath, are evaluated. The mechanism of generation of scattered waves is connected with appearance of induced charges and currents under the action of the incident EM wave. We will investigate the interaction of incident wave and low frequency turbulent pulsations inside a plasma sheath, which are assumed to be relatively small. In this case we can separate the incident and scattered waves. On the other hand, the process of the interaction of the incident wave with the turbulent plasma pulsations requires the use of nonlinear equations. The nonlinear current generated by this process in the case of a high frequency incident electromagnetic wave contains only an electron component. The dispersion properties of waves involved in the scattering process are presented in Figure 7, where the wave frequency is schematically plotted as a function of the wave number k. It follows that different scenarios are possible from the analysis of the dispersion of the electromagnetic, electrostatic Langmuir, and ion acoustic waves involved in the scattering process.

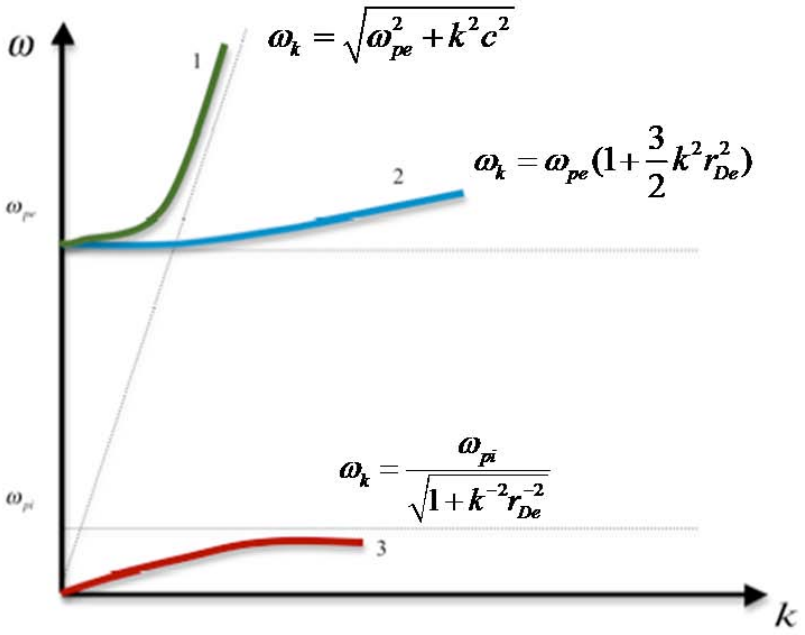

Fig. 7. Dispersion curves of waves inside the plasma sheath:

1 – electromagnetic wave with the dispersion: $\omega_k = \sqrt{\omega_{pe}^2 + k^2 c^2}$

2 – Langmuir wave with the dispersion: $\omega_k = \omega_{pe}(1 + \frac{3}{2} k^2 r_{De}^2)$, where $r_{De} = \frac{V_{Te}}{\omega_{pe}}$ is the electron Debye radius, V_{Te} is electron thermal velocity and ω_{pe} is the electron plasma frequency.

3 – Ion acoustic wave with the dispersion: $\omega_k = \frac{\omega_{pi}}{\sqrt{1 + k^{-2} r_{De}^{-2}}}$ where ω_{pi} is the ion plasma frequency.

In the case when the frequency of the incident EM wave is much larger than the electron plasma frequency ($\omega_0 >> \omega_{pe}$), the scattered waves will also be electromagnetic with frequencies in the range $\omega_0 \pm \omega_A$, where frequency ω_A belongs to the wave from the ion acoustic wave spectrum excited in the plasma flow. In the case when the frequency of the incident EM wave is close to the plasma frequency ($\omega_0 \geq \omega_{pe}$) two processes can take place:

1. Scattering of the incident EM wave into another electromagnetic wave with frequency $\omega_0 \pm \omega_A$.
2. Transformation of an incident EM wave into a Langmuir wave with frequencies in the range $\omega_0 \pm \omega_A$.

We first investigate the scattering of an incident EM wave with frequency $\omega_0 >> \omega_{pe}$. We consider a plasma sheath with the following parameters: electron density $n_{0e} = 10^8$ cm^{-3}, electron plasma frequency $\omega_{pe} = 5.64 \times 10^8$ rad/sec, ion plasma frequency $\omega_{pi} = 2.11 \times 10^6$ rad/sec, and the frequency of the incident EM wave $\omega_0 = 2\pi \times 10^9$ rad/sec. The density of the neutral air molecules inside the plasma sheath is taken to be $n_N = 10^{11}$ cm^{-3}. The scattering cross section of electrons on the neutral air molecules for the case when the electron energy does not exceed 200 eV can be taken as $\sigma_e \sim 1.5 \times 10^{-15}$ cm^2 [11]. For a temperature of electrons $T_e \sim 0.01$ eV the electron - neutral collision frequency can be estimated as: $\nu_{en} = n_N V_{Te} \sigma_e = 6.29 \times 10^2$ sec^{-1}. In this report we focus attention on the analysis of the scattering of an EM wave with *p* polarization. This wave can be presented in the following form:

$$\mathbf{E}_0 = \mathbf{E}_{0,\mathbf{k}_0} \exp\{i(\mathbf{k}_0 \mathbf{r} - \omega_{k_0} t)\} \tag{27}$$

where for the components of the electric and magnetic fields in the wave we have:

$$\mathbf{E}_0 = \{E_{0x}, E_{0y}, 0\}; \quad \mathbf{B}_0 = \{0, 0, B_{0z}\} \ . \tag{28}$$

We use the Maxwell's equations to describe the scattered waves

$$\text{rot}\, \mathbf{E}_\pm = -\frac{1}{c} \frac{\partial \mathbf{B}_\pm}{\partial t} \tag{29}$$

$$\text{rot}\, \mathbf{B}_\pm = \frac{4\pi}{c} \mathbf{j}_\pm + \frac{1}{c} \frac{\partial \mathbf{E}_\pm}{\partial t} \tag{30}$$

The current $\mathbf{j}_\pm$ contains linear and nonlinear parts:

$$\mathbf{j}_\pm = \mathbf{j}_\pm^L + \mathbf{j}_\pm^{NL} \ . \tag{31}$$

In order to find the linear current $\mathbf{j}_\pm^L$ we can use the linearized Vlasov equation for the distribution function of electrons:

$$\frac{\partial \delta f_{\pm}^{L}}{\partial t}+\mathbf{v}\cdot\frac{\partial \delta f_{\pm}^{L}}{\partial \mathbf{r}}-\frac{e}{m_e}\{\mathbf{E}_{\pm}+\frac{1}{c}[\mathbf{v}\times\mathbf{B}_{\pm}]\}\frac{\partial f_M}{\partial \mathbf{v}}=0\ . \tag{32}$$

In Equation 32 $\delta f_{\pm}^{L}$ is the linear part of the distribution function of plasma electrons associated with the electric and magnetic field of the scattered wave. f_M is the zeroth order Maxwellian distribution function:

$$f_M=\frac{n_{0e}}{(2\pi)^{3/2}V_{Te}^3}\exp\left\{-\frac{\mathrm{v}_x^2+(\mathrm{v}_y-u_{0y})^2+\mathrm{v}_z^2}{2V_{Te}^2}\right\}\ , \tag{33}$$

where u_{0y} is the flow speed.

The linear current $\mathbf{j}_{\pm}^{L}$ is the first moment of the distribution function:

$$\mathbf{j}_{\pm}^{L}=-e\int\mathbf{v}\delta f_{\pm}^{L}d^3\mathrm{v}\ . \tag{34}$$

To solve Equation 32 we will choose the system of coordinates moving together with the plasma flow:

$$\mathrm{v}_x=\hat{\mathrm{v}}_x;\quad \mathrm{v}_y=\hat{\mathrm{v}}_y-u_{0y};\quad \mathrm{v}_z=\hat{\mathrm{v}}_z \tag{35}$$

$$\mathbf{r}=\hat{\mathbf{r}}+u_{0y}t\cdot\mathbf{e}_y \tag{36}$$

where $\mathbf{v}$ and $\mathbf{r}$ are in the new coordinate system while $\hat{\mathbf{v}}$ and $\hat{\mathbf{r}}$ are in the laboratory system. In the new system of coordinates we should replace the frequency of the incident wave by the Doppler-shifted frequency:

$$\omega_0=\hat{\omega}_0-k_{0y}u_{0y}\,, \tag{37}$$

where ω is in the new system of coordinates and $\hat{\omega}$ in the laboratory system. Now it is possible to write equations for the components of the electric field in the scattered waves in the following form:

$$[\frac{\omega_{\pm}^2}{c^2}-\frac{\omega_{pe}^2}{c^2}-(k_{\pm x}^2+k_{\pm y}^2)]E_{xk_{\pm}}=-i\frac{4\pi\omega_{\pm}}{c^2}j_{xk_{\pm}}^{NL}\ , \tag{38}$$

$$[\frac{\omega_{\pm}^2}{c^2}-\frac{\omega_{pe}^2}{c^2}-(k_{\pm x}^2+k_{\pm y}^2)]E_{yk_{\pm}}=-i\frac{4\pi\omega_{\pm}}{c^2}j_{yk_{\pm}}^{NL}\ . \tag{39}$$

On introducing $\varepsilon_{\perp}(\omega_{\pm},\vec{k}_{\pm})$, defined as

$$\frac{\omega_{\pm}^2}{c^2}-\frac{\omega_{pe}^2}{c^2}-(k_{\pm x}^2+k_{\pm y}^2)=\frac{\omega_{\pm}^2}{c^2}\varepsilon_{\perp}(\omega_{\pm},\mathbf{k}_{\pm})\ , \tag{40}$$

we represent (38) and (39) as:

$$\frac{\omega_{\pm}^2}{c^2}\varepsilon_{\perp}(\omega_{\pm},\mathbf{k}_{\pm})\mathbf{E}_{\mathbf{k}_{\pm}} = -i\frac{4\pi\omega_{\pm}}{c^2}\mathbf{j}_{k_{\pm}}^{NL}. \tag{41}$$

Now we calculate the nonlinear current $\mathbf{j}_{k_{\pm}}^{NL}$ which is responsible for the scattered waves generated by the interaction of the incident EM wave with low frequency ion acoustic type perturbations. First we represent the distribution function *F* of electrons in the form

$$F = f_M + \delta f_0 + \delta f_1^{\pm} + \delta f_A, \tag{42}$$

where f_M is the Maxwell distribution given by Equation 33, δf_0 is the perturbed distribution due to the presence of the EM wave, $\delta f_1^{\pm} = \delta f_1^{\pm L} + \delta f_1^{\pm N}$ are the linear and nonlinear parts of the perturbed distribution function due to the presence of the scattered signals, and δf_A corresponds to the perturbation of the distribution function due to the presence of ion acoustic turbulence. The equation for the distribution function associated with the nonlinear generation of scattered waves has the form

$$\frac{\partial\delta f_1^N}{\partial t} + \mathbf{v}\cdot\frac{\partial\delta f_1^N}{\partial\mathbf{r}} = \frac{e}{m_e}\{\mathbf{E}_0 + \frac{1}{c}[\mathbf{v}\times\mathbf{B}_0]\}\frac{\partial\delta f_A}{\partial\mathbf{v}} + \frac{e}{m_e}\{\delta\mathbf{E}_A + \frac{1}{c}[\mathbf{v}\times\delta\mathbf{B}_A]\}\frac{\partial\delta f_0}{\partial\mathbf{v}} \tag{43}$$

In Equation 43 $\mathbf{E}_0$ and $\mathbf{B}_0$ are the wave fields of the incident EM wave, $\delta\mathbf{E}_A$ is the electric field in electrostatic ion acoustic perturbations, and $\delta\mathbf{B}_A = 0$. We use Fourier transforms to solve (43). If we take the following expression for the incident EM wave:

$$\mathbf{E}_0(\mathbf{r},t) = \mathbf{E}_{\mathbf{k}_0}\sin(\mathbf{k}_0\mathbf{r} - \omega_{\mathbf{k}_0}t), \tag{44}$$

its Fourier components are given as

$$<\mathbf{E}_0>_{k,\omega} = \frac{1}{2i}\mathbf{E}_{\mathbf{k}_0}\delta(\mathbf{k}_0 - \mathbf{k})\delta(\omega_0 - \omega) - \frac{1}{2i}\mathbf{E}_{\mathbf{k}_0}\delta(\mathbf{k}_0 + \mathbf{k})\delta(\omega_0 + \omega). \tag{45}$$

The Fourier transform for the ion acoustic waves has the form

$$\delta\mathbf{E}_{\vec{k}_A\omega_A} = \frac{1}{(2\pi)^4}\int\delta\mathbf{E}_A(\mathbf{k},t)\exp\{i(\omega_A t - \mathbf{k}_A\mathbf{r})d^3\mathbf{r}dt. \tag{46}$$

The Fourier components of the nonlinear part of the distribution function of scattered waves are given as

$$\delta f_{\mathbf{k},\omega}^N = \frac{ie}{m_e}\frac{1}{\omega - \mathbf{k}\cdot\mathbf{v}}\widehat{F}_{\mathbf{k},\omega}[(\mathbf{E}_0 + \frac{1}{c}\mathbf{v}\times\mathbf{B}_0)\frac{\partial\delta f_A}{\partial\mathbf{v}}] + \frac{ie}{m_e}\frac{1}{\omega - \mathbf{k}\cdot\mathbf{v}}\widehat{F}_{\mathbf{k},\omega}[\delta\mathbf{E}_A\frac{\partial\delta f_0}{\partial\mathbf{v}}] \tag{47}$$

In Equation 47 the operator $\widehat{F}_{\mathbf{k},\omega}$ stands for the Fourier transformation applied to the expression in the brackets.The induced plasma current due to the interaction of the incident EM wave and ion acoustic waves (responsible for excitation of scattered waves) is given by

$$\delta \mathbf{j}_{k,\omega}^{N} = -e\int \mathbf{v}\cdot\delta f_{k,\omega}^{N} d^{3}\mathbf{v}\,. \tag{48}$$

Using Equation 47 for $\delta \mathbf{j}_{k_{\pm}\omega_{\pm}}^{N}$ we obtain

$$\delta \mathbf{j}_{\mathbf{k},\omega}^{N} = \delta \mathbf{j}_{1} + \delta \mathbf{j}_{2} + \delta \mathbf{j}_{33}\ , \tag{49}$$

where

$$\delta \mathbf{j}_{1} = -\frac{ie^{2}}{m_{e}}\mathbf{v}\frac{1}{\omega - \mathbf{k}\cdot\mathbf{v}}\frac{\partial}{\partial \mathbf{v}}\int \mathbf{E}_{k_{0}\omega_{0}}\delta f_{A,\mathbf{k}-\mathbf{k}',\omega-\omega'} d^{3}\mathbf{k}' d\omega'\ , \tag{50}$$

$$\delta \mathbf{j}_{2} = -\frac{ie^{2}}{m_{e}}\int d^{3}\mathrm{v}\cdot\mathbf{v}\frac{1}{\omega - \mathbf{k}\cdot\mathbf{v}}\int \frac{1}{c}[\mathbf{v}\times\mathbf{B}_{0,k'\omega'}]\frac{\partial}{\partial \mathbf{k}}\delta f_{A,\mathbf{k}-\mathbf{k}',\omega-\omega'} d^{3}\mathbf{k}'\, d\omega'\ , \tag{51}$$

and

$$\delta \mathbf{j}_{3} = -\frac{ie^{2}}{m_{e}}\mathbf{v}\frac{1}{\omega - \mathbf{k}\cdot\mathbf{v}}\frac{\partial}{\partial \mathbf{v}}[\int \mathbf{E}_{A,\mathbf{k}'\omega'}\delta f_{0,\mathbf{k}-\mathbf{k}',\omega-\omega'} d^{3}\mathbf{k}'\, d\omega']\ . \tag{52}$$

It is possible to show that:

$$\frac{|\,\delta \mathbf{j}_{2}\,|}{|\,\delta \mathbf{j}_{1}\,|} \sim \frac{\mathbf{k}\cdot\mathbf{v}}{\omega} << 1 \tag{53}$$

and

$$|\,\delta \mathbf{j}_{3}\,| \sim \frac{e\Phi_{A}}{m_{e}c^{2}}\,|\,\delta \mathbf{j}_{\mathbf{k},\omega}^{N}\,| \ << \ |\delta \mathbf{j}_{\mathbf{k},\omega}^{N}\,|\,. \tag{54}$$

Taking into account (53) and (54) we finally have for the current which is responsible for the excitation of scattered waves

$$\delta \mathbf{j}_{k,\omega}^{N} = \frac{3ie^{2}}{m_{e}\omega}\int \mathbf{E}_{0,\mathbf{k}',\omega'}\delta n_{A,\mathbf{k}-\mathbf{k}',\omega-\omega'} d^{3}k' d\omega'\ . \tag{55}$$

Now with the help of Equation 41 we have

$$\mathbf{E}_{\mathbf{k},\omega}^{t} = \frac{3\omega_{pe}^{2}}{\varepsilon_{\mathbf{k},\omega}^{t}\omega^{2}n_{0}}\int \mathbf{E}_{0,\mathbf{k}',\omega'}\delta n_{A,\mathbf{k}-\mathbf{k}',\omega-\omega'} d^{3}k'\, d\omega'\ , \tag{56}$$

where $\mathbf{E}_{\mathbf{k},\omega}^{t}$ is the Fourier transform of the scattered electromagnetic waves, and

$$\varepsilon^{t}_{\mathbf{k},\omega} = 1 - \frac{\omega_{pe}^2}{\omega^2} - \frac{k^{\,2}c^2}{\omega^2} \quad . \tag{57}$$

The spectrum of the scattered electromagnetic field (Equation 56) in fact consists of two parts, $\mathbf{E}_{\mathbf{k}_-,\omega_-}$ and $\mathbf{E}_{\mathbf{k}_+,\omega_+}$, where

$$\mathbf{k}_{\pm} = \mathbf{k}_0 \pm \mathbf{k}_A \tag{58}$$

and

$$\omega_{\pm} = \omega_0 \pm \omega_A \tag{59}$$

In Equations 58 and 59, $\mathbf{k}_0$ is the wave vector of the incident EM signal and $\mathbf{k}_A$ is the wave vector from the turbulent spectrum of the ion acoustic waves. Using (56), (58), and (59) we obtain

$$\begin{aligned} \mathbf{E}_{\mathbf{k},\omega} &= \frac{3\omega_{pe}^2}{\varepsilon^{t}_{\mathbf{k},\omega}\omega^{\,2}n_0}\int \mathbf{E}_{0,\mathbf{k}',\omega'}\delta n_{A,\mathbf{k}-\mathbf{k}',\omega-\omega'}d^3k'd\omega' \\ &= \frac{3\omega_{pe}^2}{\varepsilon^{t}_{\mathbf{k},\omega}\omega^{\,2}n_0}\frac{\mathbf{E}_0}{2i}[\delta n^{A}_{\mathbf{k}-\mathbf{k}_0} - \delta n^{A}_{\mathbf{k}+\mathbf{k}_0}]\,. \end{aligned} \tag{60}$$

Instead of the field given by (60) we can introduce fields $\mathbf{E}^{-}{}_{\mathbf{k}_-,\omega_-}$ and $\mathbf{E}^{+}{}_{\mathbf{k}_+,\omega_+}$, where $(\mathbf{k}_-,\omega_-)$ and $(\mathbf{k}_+,\omega_+)$ are given by (58) and (59), respectively. Now, taking into account that $\varepsilon^{t}_{-\mathbf{k}_-} = \varepsilon^{*t}_{\mathbf{k}_-}$ from (60) we obtain

$$\mathbf{E}^{-}{}_{\mathbf{k}_-,\omega_-} = \frac{3}{2i}\frac{\omega_{pe}^2}{\varepsilon^{t}_{\mathbf{k}_-,\omega_-}\omega_-{}^{2}n_0}\mathbf{E}_0\delta n^{*A}_{\mathbf{k}_A,\omega_A}\,.$$

A similar expression can be obtained for $\mathbf{E}^{+}{}_{\mathbf{k}_+,\omega_+}$.The electric field in real space is given by

$$\mathbf{E}^{-} = \int d\mathbf{k}_A d\omega_A \mathbf{E}^{-}_{\mathbf{k}_-,\omega_-}\exp[i(\mathbf{k}_-\mathbf{r} - \omega_- t)\,. \tag{61}$$

From Equation 61 it is clearly seen that the spectrum of scattered waves consists of shifted wave vectors and frequencies, proportional to the wave vectors and frequencies in the spectrum of ion acoustic waves excited by a flow with velocity shear. The expression for the nonlinear current (Equation 55) can be written in the form

$$\delta \mathbf{j}^{N}_{k,\omega} = \frac{3ie^2}{m_e \omega} \int \mathbf{E}_{0,\mathbf{k}',\omega'} \delta n_{A,\mathbf{k}-\mathbf{k}',\omega-\omega'} d^3k' d\omega' \\ = \frac{3\omega_{pe}^2}{8\pi n_0 \omega} \mathbf{E}_0 [\delta n_{\mathbf{k}-\mathbf{k}_0,\omega-\omega_0} - \delta n_{\mathbf{k}+\mathbf{k}_0,\omega+\omega_0}]. \tag{62}$$

Again, from Equations 58 and 59 we get

$$\delta \mathbf{j}^{-}_{N,\mathbf{k}\_,\omega\_} = \frac{3\omega_{pe}^2}{8\pi n_0 \omega\_} \mathbf{E}_0 \delta n^{*}_{\mathbf{k}_A,\omega_A} \tag{63}$$

and $$\delta \mathbf{j}_N{}^{-} = \int d\mathbf{k}_A d\omega_A \delta \mathbf{j}^{-}_{N,\mathbf{k}\_,\omega\_} \exp[i(\mathbf{k}\_\mathbf{r} - \omega\_ t) \tag{64}$$

In order to calculate the scattered power we should define the increase in the energy of scattered waves during one second as

$$\delta Q^{-} = -\mathrm{Re} \int < \delta \mathbf{j}^{-}_N(\vec{r},t) \cdot \mathbf{E}^{-*}(\vec{r},t) > d^3r \ , \tag{65}$$

where Re means the real part, $\mathbf{E}^{-*}(\vec{r},t)$ is the complex conjugate of the scattered electromagnetic field, and <…> denotes time average. Further, using the following relations,

$$\delta \mathbf{j}^{-}_N(\vec{r},t) = \frac{3\omega_{pe}^2}{8\pi n_0} \int d\mathbf{k}\_ d\omega\_ \frac{1}{\omega\_} \mathbf{E}_0 \delta n^{*}_{\mathbf{k}_0-\mathbf{k}\_,\omega_0-\omega\_} \exp[i(\mathbf{k}\_\mathbf{r} - \omega\_ t)] \tag{66}$$

and $$\mathbf{E}^{-}(\vec{r},t) = \frac{3\omega_{pe}^2}{8\pi n_0} \int d\mathbf{k}'\_ d\omega'\_ \frac{1}{\omega'^2\_} \frac{1}{\varepsilon^{t}_{\mathbf{k}'\_,\omega'\_}} \mathbf{E}_0 \delta n^{*}_{\mathbf{k}_0-\mathbf{k}'\_,\omega_0-\omega'\_} \exp[i(\mathbf{k}'\_\mathbf{r} - \omega'\_ t)] \tag{67}$$

we finally obtain

$$\delta Q^{-} = -\frac{9\pi^{32}\omega_{pe}^4}{n^2{}_0} E_0^2 \,\mathrm{Re} \int d\mathbf{k}\_ d\omega\_ \frac{i}{\varepsilon^{t*}_{\mathbf{k}'\_,\omega'\_} \omega^3\_} |\, \delta n^{*}_{\mathbf{k}_0-\mathbf{k}\_,\omega_0-\omega\_} \,|^2 \tag{68}$$

with the density spectrum defined as

$$|\, \delta n_{k_{Ax},k_{Ay},\omega_A} \,|^2 = \frac{A}{(k_{Ax}^2 + k_{Ay}^2)^2} \frac{1}{\omega_A^2},$$

where $A \sim 0.1$, based on our numerical results.

Knowledge of (68) allows us to calculate the scattering cross section σ^{-} due to the presence of ion acoustic turbulence as

$$\sigma^{-} = \frac{\delta Q^{-}}{c \dfrac{E_0^2}{4\pi}} \ , \tag{69}$$

where σ^- is defined as the ratio of the scattered power (defined as the work done per unit time by the field created by the nonlinear current) to the energy flux of the incident EM signal. From Equation 68 we see that it is necessary to include dissipative terms in the expression for $\varepsilon^t_{\mathbf{k},\omega}$, otherwise $\delta Q^- = 0$. Taking into account collisions of electrons with neutrals we have

$$\varepsilon^t{}_{\mathbf{k},\omega} = 1 - \frac{\omega_{pe}^2}{\omega^2} - \frac{k^2c^2}{\omega^2} + i\frac{\nu_{en}\omega_{pe}^2}{\omega^3}$$

$$\varepsilon^t{}_{1,\mathbf{k},\omega} = 1 - \frac{\omega_{pe}^2}{\omega^2} - \frac{k^2c^2}{\omega^2} \qquad \varepsilon^t{}_{2,\mathbf{k},\omega} = i\frac{\nu_{en}\omega_{pe}^2}{\omega^3}.$$

Now we can write

$$\mathrm{Re}\left(\frac{i}{\varepsilon^{t*}{}_{\mathbf{k},\omega}}\right) = -\frac{\varepsilon^t{}_{2,\mathbf{k},\omega}}{(\varepsilon^t{}_{1,\mathbf{k},\omega})^2 + (\varepsilon^t{}_{2,\mathbf{k},\omega})^2}\ . \tag{70}$$

There are two ways to calculate the integral in (68). In the first case, which we can call non-resonance, scattered waves are not plasma eigenmodes, i.e.,

$$\varepsilon_1^t(\omega_\pm, \mathbf{k}_\pm) \neq 0\ , \tag{71}$$

and this results in

$$\omega_\pm \neq \omega_{\mathbf{k}_\pm}\ . \tag{72}$$

In the second instance, the resonance case, we have

$$\varepsilon_1^t(\omega_\pm, \mathbf{k}_\pm) \sim 0 \tag{73}$$

and [5, 6]

$$\mathrm{Re}\left(\frac{i}{\varepsilon^{t*}{}_{\mathbf{k},\omega}}\right) = -\pi\frac{\delta(\omega_- - \omega_{k_-})}{\left.\frac{\partial\varepsilon_1^L}{\partial\omega_-}\right|_{\omega_- = \omega(k_-)}}\ . \tag{74}$$

It follows from the dispersion properties of the EM and ion acoustic waves that (for the range of frequencies and plasma parameters of interest) we should consider the non-resonance case (Equation 71). Using (70) in the integral for the scattering cross section given in (69) and performing the numerical integration one obtains the following results. When the width of the plasma sheath is varying in the interval

$$3 < L_x < 15 \text{ cm} \tag{75}$$

the amplitude of the scattered waves is found to belong to the interval

$$10^{-5} < \frac{E_{\pm}}{E_0} < 10^{-1} , \quad (76)$$

where E_0 is the amplitude of the incident EM wave. The corresponding scattering cross sections belong to the interval:

$$10^{-17} < \sigma^{\pm} < 10^{-8} \text{ cm}^2 \quad (77)$$

It is also worth mentioning that the phase change in the scattered waves can impact the phase-locking-in process for signals from GPS satellites. This is connected with the fact that the absolute values of the wave vectors of scattered waves $\mathbf{k}_{\pm} = \mathbf{k}_0 \pm \mathbf{k}_A$, due to the inequality $k_0 \ll \mathrm{k}_A$, can be responsible for a significant change of the integrated phase shift $\psi \sim \int k_{\pm} dx$.

4. TRANSFORMATION TO LANGMUIR WAVES

Below we present an analysis of the transformation of the incident EM signal into a Langmuir wave due to interaction with density perturbations associated with ion acoustic turbulence excited by a plasma flow with velocity shear around a hypersonic vehicle. The transformation process can take place when the frequency of the incident EM signal is close to the electron plasma frequency inside the sheath. This corresponds to an electron plasma density $n_e \sim 10^{10}\ cm^{-3}$. The efficiency of the transformation of an EM wave (in our case it is the GPS signal) propagating through a plasma sheath into an electrostatic Langmuir wave on ion acoustic density perturbations will be evaluated. We also show that inside the plasma sheath the process of transformation is resonant in nature, in contrast to the EM signal scattering into an electromagnetic wave. As a result the excited wave amplitudes as well as the scattering cross section for this process are much larger than the corresponding quantities in the case of scattering into an electromagnetic wave.

The mechanism of appearance of electrostatic Langmuir waves is connected with transformation of an incident EM wave on ion acoustic density perturbations by induced charges and currents. So in the process of this interaction another type of wave – an electrostatic Langmuir wave – is generated and this is the reason it is called a wave transformation.

Dispersion properties of waves involved in the scattering process are presented in Figure 1. Below we concentrate on the case when $\omega_0 \geq \omega_{pe}$ (frequency of the EM wave is slightly above the plasma frequency inside the sheath) and transformation of the EM signal into an electrostatic Langmuir wave on ion acoustic density perturbations is possible. We will consider a plasma sheath with the following parameters: electron density $n_{0e} \sim 10^{10}$ cm^{-3}, so that the electron plasma frequency is slightly smaller than the frequency of the incident EM wave (GPS signal $\omega_0 \sim 2\pi \times 10^9$ rad / sec). The density of neutral air molecules inside the plasma sheath is taken to be $n_N = 10^{11}$ cm^{-3}. As in the previous section, we analyze the scattering of an electromagnetic wave with *p* polarization (see (28)).

The scattered Langmuir wave being an electrostatic wave, will have the following polarization:

$$\mathbf{E}_1 = \{E_{1x}, E_{1y}, 0\}; \quad \mathbf{B}_1 = \{0,0,0\}. \tag{78}$$

To describe the scattered wave we use the Poisson equation:

$$div\mathbf{E}_{\pm} = -4\pi e n^{\pm}, \tag{79}$$

where $\mathbf{E}_{\pm} = -\nabla\Phi^{\pm}$ and $\Delta\Phi^{\pm} = 4\pi e n^{\pm}$ (80)

The density $n^{\pm}$ contains linear and nonlinear parts

$$n^{\pm} = n_L^{\pm} + n_{NL}^{\pm}. \tag{81}$$

In order to find the linear density perturbation $n_L^{\pm}$ we use the linearized Vlasov equation for the distribution function of the electrons:

$$\frac{\partial \delta f_{\pm}^L}{\partial t} + \vec{\mathrm{v}} \cdot \frac{\partial \delta f_{\pm}^L}{\partial \vec{r}} - \frac{e}{m_e} \vec{E}_{\pm} \frac{\partial f_M}{\partial \vec{\mathrm{v}}} = 0 \ . \tag{82}$$

In equation (82) $\delta f_{\pm}^L$ is the linear part of the distribution function of plasma electrons associated with the electric field of the scattered wave. f_M denotes the zeroth-order Maxwellian distribution function defined as

$$f_M = \frac{n_{0e}}{(2\pi)^{3/2} V_{Te}^3} \exp\{-\frac{\mathrm{v}_x^2 + (\mathrm{v}_y - u_{0y})^2 + \mathrm{v}_z^2}{2V_{Te}^2}\} \tag{83}$$

where u_{0y} is the flow speed. The linear density perturbation $\delta n_L^{\pm}$ is the zero-th order moment of the distribution function given as

$$n_L^{\pm} = \int \delta f_L^{\pm} d^3\mathrm{v} \ . \tag{84}$$

To solve (79) we, as in the previous section, choose the system of coordinates moving together with the plasma flow, and hence obtain

$$\delta f_{\mathbf{k}_{\pm}}^L = -\frac{e n_{0e}}{m_e} \frac{\mathbf{k}_{\pm} \cdot \mathbf{v}}{\omega_{\mathbf{k}_{\pm}} - \mathbf{k}_{\pm} \cdot \mathbf{v}} \Phi_{\mathbf{k}_{\pm}} \cdot f_M \tag{85}$$

and

$$n_{\mathbf{k}_{\pm}}^L = \int \delta f_{\mathbf{k}_{\pm}}^L d^3\mathrm{v} = -\frac{e n_{0e} \Phi_{\mathbf{k}_{\pm}}}{(2\pi)^{3/2} \mathrm{v}_{Te}^5 m_e} \int \frac{\mathbf{k}_{\pm} \cdot \mathbf{v}}{\omega_{\mathbf{k}_{\pm}} - \mathbf{k}_{\pm} \cdot \mathbf{v}} \exp[-\frac{\mathrm{v}_x^2 + \mathrm{v}_y^2 + \mathrm{v}_z^2}{2\mathrm{v}_{Te}^2}] d^3\mathrm{v} \ , \tag{86}$$

where $n_{\mathbf{k}_{\pm}}^L$ represents the linear part of the density fluctuations. After substituting (86) into (4) we finally write the Poisson equation as

$$\varepsilon^L(\mathbf{k}_{\pm}, \omega_{\pm}) k_{\pm}^2 \Phi_{\mathbf{k}_{\pm}} = -4\pi e n_{\pm}^{NL} \ , \tag{87}$$

where

$$\varepsilon^L(\mathbf{k}_{\pm}, \omega_{\pm}) = 1 + \frac{1}{k_{\pm}^2 r_{De}^2} [1 + i\sqrt{\pi} z w(z)], \tag{88}$$

with $w(z)$ defined as

$$w(z) = \frac{i}{\pi} \int_{-\infty}^{\infty} \frac{\exp(-y^2)}{z - y} \tag{89}$$

and

$$z_{\pm} = \frac{\omega_{\pm}}{\sqrt{2} k_{\pm} \mathrm{v}_{Te}} \qquad t = \frac{\mathrm{v}}{\sqrt{2}\mathrm{v}_{Te}} \ . \tag{90}$$

Finally, the Fourier component of the scattered Langmuir wave field can be written as

$$\mathbf{E}_{\mathbf{k}_-, \omega_-} = -i\mathbf{k}_- \Phi_{\mathbf{k}_-} = -\frac{3i}{2} \frac{1}{n_0} \frac{\omega_{pe}^2}{\omega_-^2} \frac{1}{\varepsilon^L(\mathbf{k}_-, \omega_-)} \frac{(\mathbf{k}_- \cdot \mathbf{E}_0)}{k_-^2} \delta n_{\mathbf{k}_A, \omega_A}^* \mathbf{k}_- \ . \tag{91}$$

Hence we obtain the following expression for the scattering cross section:

$$\sigma_L^- = \frac{36\pi^4\Delta_i^2}{c}\left(\frac{M_i}{m_e}\right)^2 \int dk_{Ax}dk_{Ay}d\omega_A \frac{(k_{Ax}\cos\theta_0 + k_{Ay}\sin\theta_0)^2}{k_-^2} \times \frac{1}{(\omega_0-\omega_A)^3}\frac{\varepsilon_2^L}{|\varepsilon_1^L|^2+|\varepsilon_2^L|^2}|\delta n_{k_{Ax},k_{Ay},\omega_A}|^2 . \tag{92}$$

Taking into account that scattered Langmuir waves are now the plasma eigenmodes, we make use of expression (74) in Equation 92. Also we use the following expression for the scattering cross section for the numerical integration:

$$\sigma_{L\,res}^- = 18\pi^5 \frac{1}{\tilde{c}}\frac{\tilde{V}_{Te}^2}{\tilde{\omega}_{pi}^2}\int\int dk_{-,x}dk_{-,y}\frac{(k_{Ax}\cos\theta_0 + k_{Ay}\sin\theta_0)^2}{k_-^2}|\delta n_{\vec{k}_0-\vec{k}_-,\omega_0-\omega_{\vec{k}_-}}|^2, \tag{93}$$

with the density spectrum defined as

$$|\delta n_{k_{Ax},k_{Ay},\omega_A}|^2 = \frac{A}{(k_{Ax}^2+k_{Ay}^2)^2}\frac{1}{\omega_A^2} , \tag{94}$$

where according to numerical results $A \sim 0.1$. Now, when the width of the plasma sheath is within the interval

$$3 < L_x < 15 \text{ cm} \tag{95}$$

the amplitudes of the scattered Langmuir waves are found to be much larger in comparison with the amplitude of the scattered EM waves. The ratio of the scattered Langmuir wave amplitude $E_\pm^L$ to the amplitude E_0 of the incident EM wave was found to be in the interval

$$10^{-2} < \frac{E_\pm^L}{E_0} < 1 . \tag{96}$$

Corresponding scattering cross sections are in the interval

$$10^{-5} < \sigma_L^\pm < 10^{-3} \text{ cm}^2 . \tag{97}$$

5. SUMMARY

The purpose of the work is to understand the influence of a plasma flow with velocity shear on the properties of incident EM waves used for communication purposes. This report consists of two parts. In the first part we have investigated the excitation of low frequency turbulence inside a plasma flow with velocity shear. We have demonstrated that the flow with a Gaussian velocity profile excites low frequency turbulence associated with appearance of the vortices and electrostatic ion acoustic type oscillations. In the second part of the report we analyzed the scattering of an incident EM wave on excited turbulent pulsations associated with the ion acoustic type waves. It is shown that in the case when the frequency of the incident EM wave is much greater than the electron plasma frequency, the scattered waves will be also electromagnetic with frequencies in the range $\omega_0 \pm \omega_A$, where the frequency ω_A belongs to the wave from the ion acoustic wave spectrum excited in the plasma flow. The scattered EM waves in this case are not plasma eigenmodes and can exist only as forced perturbations in the vicinity of the region where they were generated. It is also worth mentioning that a similar type of scattering (only with different type of waves involved) was observed during the active experiments in the ionospheric plasma, analyzed in [12, 13].

In the case when the frequency of the incident EM wave is close to the plasma frequency ($\omega_0 \geq \omega_{pe}$) two processes can take place:

1. Scattering of the incident EM signal into an electromagnetic wave with frequencies $\omega_0 \pm \omega_A$.
2. Transformation of an incident EM wave into Langmuir waves with frequencies in the range $\omega_0 \pm \omega_A$.

The scattered EM waves in this case are not plasma eigenmodes, but the Langmuir waves are. As a result the scattering cross section for the processes involving Langmuir waves inside a plasma sheath is much higher.

REFERENCES

[1] R.A. Hartunian, G.E. Stewart, S.D. Fergason, T.J. Curtiss and R.W. Seibold, "Causes and mitigation of radio frequency blackout during reentry of reusable launch vehicles", *Aerospace Report* ATR-2007(5309)-1, The Aerospace Corporation, Jan. 2007.

[2] T.C. Lin and L.K. Sproul, "Influence of reentry turbulent plasma fluctuation on EM wave propagation", *Computers & Fluids*, vol. 35, no 7, pp. 703-714, Aug. 2006.

[3] F.H. Mitchell, Jr., W.R. Mahaffey, R.F. Jacob, "Modeling plasma effects on radar cross section of reentry vehicles", *IBM J. Res. Develop*., pp. 468 – 474, July 1969.

[4] Yu. I. Alpert and I.P. Pitaevskii, "Scattering of electromagnetic waves by inhomogeneities excited in a plasma by a rapidly moving body", *AIAA Journ.,* vol. 1, no 4, pp. 1001 – 1009, Apr. 1963.

[5] A.I. Akhiezer, *Plasma Electrodynamics*, Elsevier, 1st English ed., April 1975.

[6] R. Bingham, U. de Angelis, V.N. Tsytovich and O. Havnes, "Electromagnetic wave scattering in dusty plasmas", *Phys. Fluids,* vol. B3, no 3, pp. 811–817, March 1991.

[7] D. Anderson, J. C. Tannehill, and R. H. Fletcher, *Computational Fluid Mechanics, and Heat Transfer*, Taylor and Francis, 1984, Chapter IV.

[8] D. Potter, *Computational Physics*, *John* Wiley & Sons, 1977, Chapter III.

[9] J. M. Dawson, "Particle simulation of plasmas," *Rev. Mod. Phys.* 55, pp 403, 1983.

[10] J. D. Jackson, *Classical Electrodynamics*, John Wiley & Sons, 1962, Chapter II.

[11] K.I. Bakhov, L.P. Babich, and I.M. Kutsyk, "Temporal characteristics of runaway electrons in electron-neutral collision-dominated plasma of dense gases," *IEEE Trans. Plasma Science,* vol. 28, no. 4, August 2000.

[12] V.I. Sotnikov, V. Fiala, F. Lefeuvre, and D. Lagoutte, "Excitation of sidebands due to nonlinear coupling between a VLF transmitter signal and a natural ELF emission," *J. Geophys. Res.*, vol. 96, A7, pp. 11363-11369, 1991.

[13] V.I. Sotnikov, D. Schriver, M. Ashour-Abdalla, and J. Ernstmeyer, "Excitation of sideband emissions by a modulated electron beam during the CHARGE-2B mission," *J. Geophys. Res.,* vol. 99, pp. 917-8923, 1994.